Article

Numerical Simulation of Heat Transfer of Roller Slag in Centrifugal Preparation of Inorganic Fiber

Chunyu Liu [1], Weixing Wang [2], Xiwei Qi [1,*], Baoxiang Wang [3,*], Wei Chen [1], Kai Zhao [1], Jie Zhen [1] and Qiaorong Zhang [1]

[1]   College of Metallurgy and Energy, North China University of Science and Technology, Tangshan 063210, China; leochunyu@foxmail.com (C.L.); hblgdxzzb@163.com (W.C.); herozk81@163.com (K.Z.); herozqr@163.com (Q.Z.)

[2]   Department of Computer Science, The University of Sheffield, Sheffield S10 2TN, UK; 13230565596@163.com

[3]   College of Materials Science and Engineering, North China University of Science and Technology, Tangshan 063210, China

*   Correspondence: qixiwei@ncst.edu.cn (X.Q.); wbxchw@163.com (B.W.)

Abstract: The synergistic preparation of aluminum silicate ceramic fibers from dust removal ash and fly ash is a newly developed process that achieves green and high added value treatment of solid waste. In this process, the centrifugal fiber forming method is used to treat molten slag to obtain aluminum silicate ceramic fibers. During the production process, the centrifugal roller, as a key component in fiber forming, is in long-term contact with high-temperature slag. The heat transfer between the two causes a huge temperature gradient inside the roller material, causing significant thermal stress inside the material, which has a significant impact on the stability of the centrifugal roller structure and its working condition. This article mainly conducts numerical simulation research on the heat transfer between the roller and the slag during the centrifugal fiber forming process, providing theoretical support for ensuring the structural stability of the roller and improving its service life. The research was carried out using the FLUENT module of the ANSYS software (V2021R1), and the heat transfer model of the slag and roller was established. The effects of the internal circulating water, different slag temperatures, different slag film widths, and different boundary layer thicknesses on the heat transfer of the roller were analyzed. The results show that the water temperature at the outlet is about 6 °C higher than that at the inlet on average; when the temperature of the slag increases by 1 °C, the temperature of the roller surface in contact with the slag increases by 0.91 °C; when the width of the slag on the roll surface is 11–17 mm and the slag thickness (boundary layer thickness) is less than 1 mm, it is beneficial for fiber production.

Keywords: centrifugal fiber; roller wheel; heat transfer; numerical simulation

1. Introduction

Inorganic fibers are widely used as insulation materials in fields, such as in architecture, furnaces, aerospace [1–4], rock wool (using basalt and coke as the raw materials), mineral wool (using blast furnace slag, ferroalloy slag, coke, etc. as the raw materials) [5], and ceramic cotton (using fly ash, dust removal ash, coke, etc. as raw the materials). At present, the main method for the industrial production of inorganic fibers is centrifugation, with the core equipment being a multi-roll centrifuge (available in two rollers and four rollers [6]). The process of synergistic preparation of aluminum silicate ceramic fibers from dust removal ash and fly ash uses a two-roller centrifuge. After the high-temperature slag (up to 1650 °C) contacts the high-speed rotating roller, under the action of viscous and friction force, the melt spreads on the roller surface and forms a liquid film with a certain thickness. In the process of the liquid film, accompanied by the rotation of the roller, the fluid instability (Kelvin–Helmholtz instability [7] and Rayleigh–Taylor instability [8]) causes the disturbance of the liquid film surface. Subsequently, the disturbance gradually

intensifies with the rotation of the liquid film and leads to the decomposition of the liquid film on the roller surface. The decomposed liquid film will stretch and pull to form liquid filaments under the action of viscosity and surface tension, and the liquid filaments will form fiber filaments of 3–10 microns after cooling and curing. However, the contact between the outer surface of the roller and the high-temperature slag during the centrifugal fiber forming process can lead to an increase in the surface temperature, adhesion of high-temperature slag, and deformation or even melting of the roller surface, which not only affects the quality and production of the fiber, but also significantly reduces the service life of the roller, increases the probability of safety accidents, and has adverse effects on production. In order to ensure the working state and structural stability of the roller, it is necessary to perform forced cooling on the roller used for centrifugal fiber forming. The usual method is to introduce circulating cooling water internally to cool the roller and maintain the normal operation of the entire centrifugal fiber forming process. The centrifugal fiber forming process and the structure of the roller water cooling system are shown in Figure 1, which results in a huge temperature gradient from the outer surface to the inner surface of the roller material, forming significant thermal stress, and ultimately causing high-temperature failure of the material as shown in Figure 2.
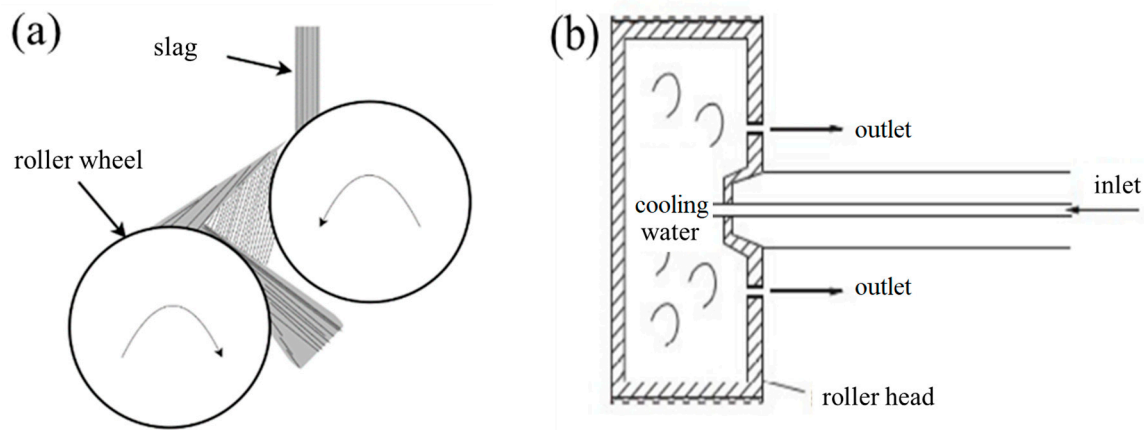

Figure 1. (**a**) Structure diagram of centrifugal fiber forming process; (**b**) roller water cooling system.

Figure 2. Roller wheel after high temperature failure (SUS304).

Although centrifugal fiber forming machines have a wide range of applications, there are few public reports on the research and modeling of these special types of rotating devices (rollers). Širok et al. [9] conducted high-speed camera visualization of molten films on industrial spinning machine rollers, analyzing the speed, and structural dynamics of early fibrosis stages. Lin Yihan et al. [10] established control differential equations and studied the rigid clamping model of four roller wheels. Jia Cili et al. [11] studied the heat treatment process of roller wheels using 2Cr13 as a raw material. Chen Jiu et al. [12] analyzed the structural design of the roller part and carried out statics analyses and strength checks on the main support arm system of the roller. Ma Wenxin et al. [13] applied ANSYS FLUENT software(V2019R1) to numerically simulate the steady-state heat transfer process of the film on a cooling drum, solving the problem of the heat transfer simulation at the

moving boundary of the film. Chang Lingling et al. [14] used numerical calculation methods to calculate the temperature field of aluminum foil cooling and analyzed the variation patterns of aluminum foil cooling. Li Fushen et al. [15] conducted numerical simulations of the cooling process of the plastic film on the casting roller and obtained the temperature variation pattern of the casting roller surface. Li Yongkang et al. [16] simulated the heat flow distribution of the cooling roller and obtained the temperature field distribution of the inner and outer walls of the cooling roller. Based on FLUENT and ANSYS, Wu Shixin [17] established relevant mathematical models for new-type cooling rolls in the secondary cold and dry cooling process of slab continuous casting. The temperature field of the bearing seat of the continuous casting roller was analyzed by Dai Wei [18] using ANSYS. Based on the research and analysis of the service life of the cast roll, Li Shande [19] carried out coupling modeling and solving analysis of the thermal structure of the roll sleeve in the continuous casting and rolling process based on ANSYS.

At present, the actual production process control of the inorganic fibers mainly relies upon experience. There is no theoretical support for the determination and optimization of the various parameters in the centrifugal fiber forming process, such as the slag temperature, slag width, and thickness. Therefore, the FLUENT module is applied using the ANSYS software (V2021R1) to numerically simulate the heat transfer behavior of the centrifugal spinning roller and the slag in a collaborative preparation of the ceramic fibers from dust removal ash and fly ash, determining the impact of the heat transfer behavior on the roller, and revealing the temperature field changes of the roller and high-temperature slag during the spinning process. Combining theory with practice, along with considering the actual production and numerical simulation situation of the enterprise, can provide technical support for the maintenance of production process rollers and optimization of the cooling process parameters.

2. Building the Model

2.1. Roller Device and Geometric Parameters

The roller device studied in this article includes one water inlet, six water outlets, and an intermediate rotating bearing. The middle rotating-bearing is installed on the driving motor, which drives the roller to rotate through the rotating bearing, achieving the process of slag centrifugation and fiber formation on the roller. The actual diagram is shown in Figure 3, and the structural parameters of the roller are shown in Table 1. Among them, the surface of the roller in direct contact with the slag in the circumferential direction is called the roller surface, the circular surface where the inlet and outlet are located is called the inner end face, and the symmetrical circular surface is called the outer end face. From the figure, it can be seen that the middle rotating bearing is a hollow bearing, that is, the bearing simultaneously serves as the water inlet, and the six water outlets are evenly distributed around the periphery of the bearing.
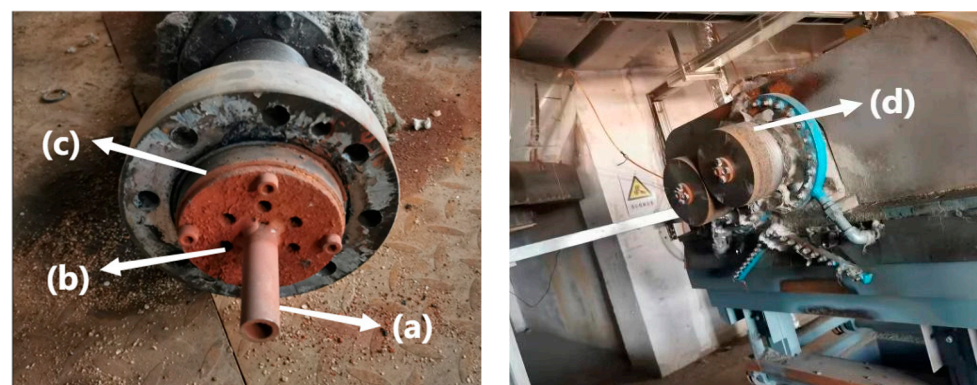

Figure 3. Roller physical diagram (a) water inlet; (b) water outlet; (c) rotating-bearing; (d) roller.

Table 1. Roller structure parameters.

Parameter	Value
Wall thickness/mm	30
Cavity diameter/mm	240
Cavity height/mm	80
Overall diameter/mm	300
Overall height/mm	140
Inlet diameter/mm	12
Outlet diameter/mm	7

Based on the internal structure and structural parameters of the roller, a three-dimensional model is created using the DesignModeler module in the ANSYS software (V2021R1). The model is divided into four parts from inside to outside: internal circulating water, roller, slag, and air. The calculation domain of the circulating water is located in the internal cavity of the roller; the outer part is a roller entity; there is a layer of slag outside the roller body, and the slag thickness is calculated according to the boundary layer equation; the outside of the slag is set as the air calculation domain, considering the heat exchange between the slag and the air. The internal circulating water, slag, and air are used as fluids, and the rollers are used as solids. The three-dimensional model of the geometric structure is shown in Figure 4.
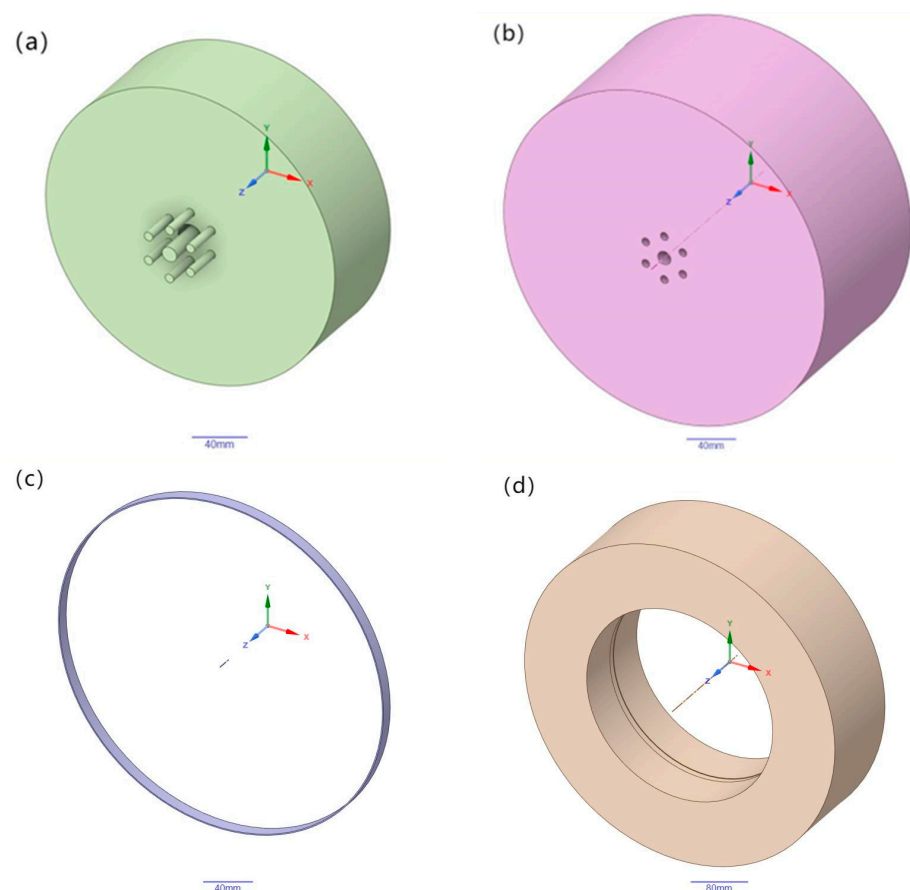
Figure 4. Three dimensional model of geometric structure (**a**) internal circulating water; (**b**) roller; (**c**) slag; (**d**) air.

2.2. Mathematical Model of Heat Transfer

2.2.1. Basic Assumptions

In practical situations, the slag undergoes heat exchange with the circulating cooling water through the rollers. At the beginning, the slag, rollers, and circulating cooling water are in an unstable state, and the temperature changes over time. After the equipment has been running for a period of time, the heat exchange between the slag, roller, and circulating cooling water reaches a dynamic balance, that is, the temperature of the roller basically does not change, and the heat released by the slag is equal to the heat absorbed by the circulating cooling water, achieving a stable state.

This article studies the heat transfer changes when the three reach a stable state, adopting steady-state calculations, namely $\partial/\partial\tau = 0$. In order to simplify the calculation model and obtain the key influencing factors, the following reasonable assumptions are made for the centrifugal fiber forming process:

(1)　The heat of the slag is only transmitted to the rollers and air;
(2)　The slag has good contact with the roller, and the gap distance approaches 0 infinitely;
(3)　The thermophysical parameters of the roller material are isotropic and do not change with temperature changes;
(4)　The difference in heat dissipation at various positions on the circumference is negligible, assuming that the roller has no circumferential heat transfer;
(5)　During simulation, the wall is non sliding and no inertial force is calculated;
(6)　Do not consider the thermal effects caused by viscous dissipation during fluid flow;
(7)　The slag can form a film on the centrifugal roller surface and the film does not break.

2.2.2. Governing Equation

The flow of slag and cooling water in the roller follows the three most basic conservation laws, namely the conservation of mass, the conservation of momentum, and the conservation of energy. This paper treats the slag and circulating cooling water as a three-dimensional steady-state incompressible fluid and adopts the continuity equation to represent the conservation of mass, the Navier–Stokes equation to represent the conservation of momentum, and the energy conservation equation to represent the conservation of energy; for the heat transfer between the slag and the roller contact surface, temperature boundary conditions are applied, on the other hand, for the heat transfer between the slag and the air-contact surface, convection boundary conditions are used.

Continuity equation:

$$\frac{1}{\rho}\frac{d\rho}{d\tau} + \frac{\partial v_x}{\partial x} + \frac{\partial v_y}{\partial y} + \frac{\partial v_z}{\partial z} = 0 \tag{1}$$

ρ is the fluid density, kg/m^3; τ is time, s; v_x, v_y, and v_z is the fluid flow rate in the x, y, and z directions, respectively, m/s.

Navier–Stokes equation is as follows:

$$\frac{dv_x}{d\tau} = X - \frac{1}{\rho}\frac{\partial p}{\partial x} + \eta\nabla^2 v_x$$

$$\frac{dv_y}{d\tau} = Y - \frac{1}{\rho}\frac{\partial p}{\partial y} + \eta\nabla^2 v_y \tag{2}$$

$$\frac{dv_z}{d\tau} = Z - \frac{1}{\rho}\frac{\partial p}{\partial z} + \eta\nabla^2 v_z$$

X, Y, and Z are forces per unit mass acting on the fluid, N; $\frac{\partial p}{\partial x}$, $\frac{\partial p}{\partial y}$, and $\frac{\partial p}{\partial z}$ are pressure gradients, Pa; η is the kinematic viscosity coefficient, m^2/s; ∇^2 is the Laplace operator.

The energy conservation equation is as follows:

$$\frac{\partial(\rho E)}{\partial \tau} + div(\rho \mu T) = div\left(\frac{\lambda}{\rho c_p} gradT\right) + S_h \tag{3}$$

E is the sum of kinetic energy, internal energy, and potential energy of the fluid micro-clusters, J/kg; T is the temperature, K; λ is the thermal conductivity, W/(m·K); S_h is the volumetric heat source term.

2.2.3. Selection of Internal Circulating Water Model

The Reynolds number is usually a measure of the typical size of the inertial force and viscous force. A high Reynolds number indicates that the inertial forces in the fluid are greater than the viscous forces, making it more prone to turbulent flow; conversely, a low Reynolds number signifies that the inertial forces are smaller than the viscous forces, making laminar flow more likely to occur.

Known data: ρ is the fluid density: 997 kg·m^{-3}; η is the kinematic viscosity: 0.897×10^{-6} m^2·s^{-1}; d_s is the inlet diameter: 12 mm; and the flow rate Q, at the internal circulating water inlet is 60 L/h, so the flow rate at the internal circulating water inlet is 0.147 m/s, and the Reynolds number is 1967.

The critical Reynolds number varies with the shape of the fluid region. Generally, according to the size of the Reynolds number, the flow state can be divided into three types [20,21]:

(1)   When Re < 2300, the flow exhibits laminar flow;
(2)   When 2300 < Re < 4000, the flow pattern is unstable, which may be laminar or turbulent, known as the transition zone;
(3)   When Re > 4000, the flow exhibits turbulence.

Based on the above analysis, the laminar flow model is selected for the internal circulating water flow model, and the laminal model is selected for the FLUENT solution. This model can set the flow state in the calculation domain to the laminar flow. The enhanced wall treatment method from FLUENT is selected for the wall treatment method, which is suitable for low Reynolds number models.

2.3. Mesh Generation

Mesh generation refers to dividing a spatially continuous computational domain into sufficiently small computational regions, fluid control equations are then applied to each of these regions to solve and calculate the fluid equations for all the regions, ultimately obtaining the distribution of physical quantities across all computational regions. In order to ensure the quality of the mesh generation and to improve the accuracy and speed of the numerical calculations, the geometric structure needs to be divided into four parts during the mesh generation, namely the internal circulating water, rollers, slag, and air, which need to be grid divided in sequence. The mesh module is used to divide the mesh, and the geometric size adjustment and boundary layer meshing are added to improve the mesh quality. The mesh type is a tetrahedral/hexahedral hybrid mesh.

In order to ensure the reliability of the model grid, we conducted experiments on grid convergence; the average mesh size of the model is divided into 5 mm, 6 mm, 7 mm, 8 mm, and 9 mm. The temperature of the line on the roller surface, which is parallel to the roller axis is taken as the entry point to verify the grid independence. The results are shown in Figure 5, which shows that the temperature has a weak dependence on the mesh size. The global average size of 9 mm is selected for the grid division of the model to strike a balance between computational accuracy and efficiency. The final number of the grid nodes is 89,137, and the number of grid units is 435,446. The grid cell quality of this model ranges from 0.7 to 1, and the average cell quality of the grid is 0.79224, which indicates that the quality of the grid delineation is good enough for a numerical simulation. The detailed meshing is shown in Figure 6.
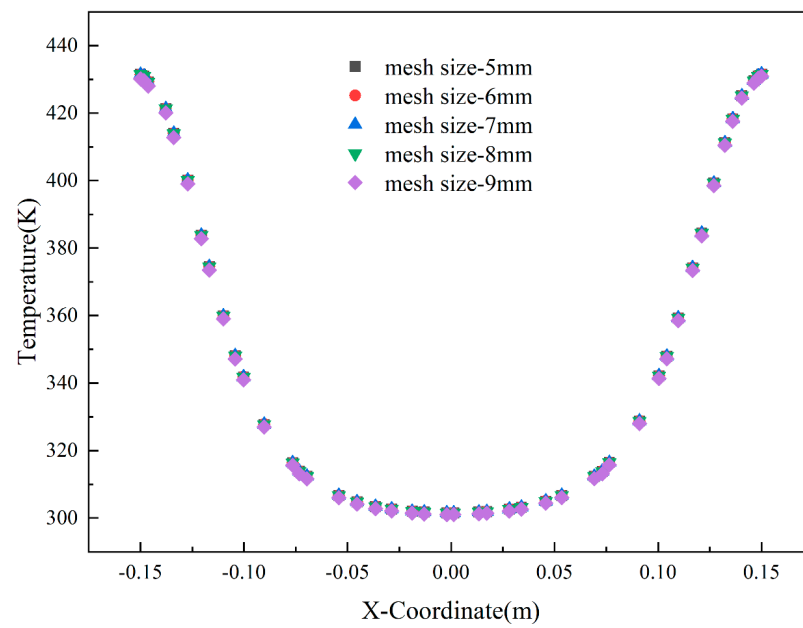
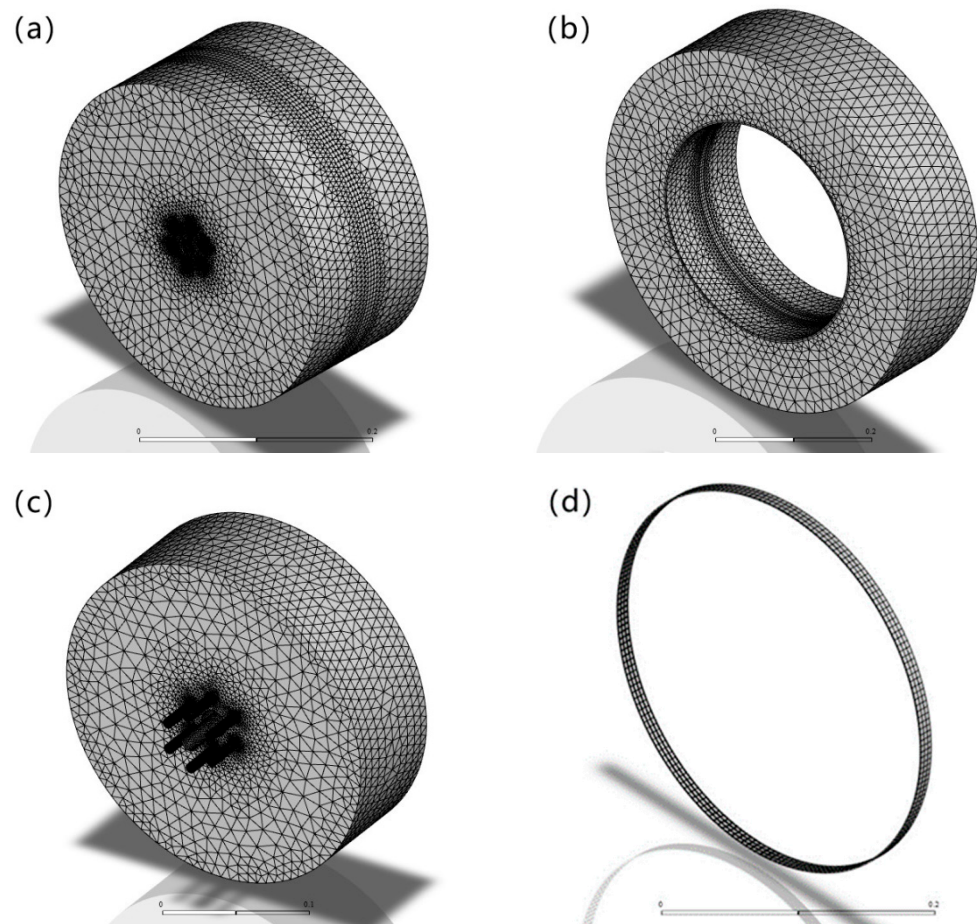**Figure 5.** The effect of different mesh sizes on temperature.

Figure 6. Mesh generation (**a**) roller; (**b**) air; (**c**) internal circulating water; (**d**) slag.

2.4. Material Property Settings

The slag, rollers, and material properties for the internal circulating cooling water in the FLUENT material database are defined and shown in Table 2.

Table 2. Slag and roller material properties.

Material	Density (kg·m^{-3})	Specific Heat Capacity (J·kg^{-1}·K^{-1})	Thermal Conductivity (W·m^{-1}·K^{-1})	Dynamic Viscosity (kg·m^{-1}·s^{-1})
slag	2500	913.11	1.5	11.421
roller wheel	7750	484.96	25.1	
circulating cooling water	998.2	4182	0.6	0.001003

2.5. Boundary Condition Settings

(1)   The inlet and outlet of the internal circulating cooling water adopt pressure boundary conditions with the inlet pressure set to 0.25 MPa, the outlet pressure set to 0.2 MPa, and the inlet temperature set to 25 °C;

(2)   The slag temperature is set to 1500 °C, the slag width is 11 mm, and the boundary layer thickness is 1.04 mm;

(3)   The slag and the roller undergo conduction heat transfer, while the slag and air undergo convective heat transfer;

(4)   The initial air temperature is set to 25 °C.

2.6. Solving Control

The SIMPLEC algorithm is selected, which is suitable for most conventional incompressible flow problems and can quickly obtain convergence solutions in the laminar flow. The steady-state solution is adopted in the solution process, and the second-order upwind scheme is used to calculate the spatial discrete scheme. The relaxation factor and residual control remain at the default settings. In order to make efficient use of the arithmetic power and to ensure the accuracy of the calculation, the residuals of the continuous and velocity terms in the calculation are set to 10^{-2}, while the residuals of the key energy term are set to 10^{-6}, which is a setup that can maintain the computational speed of the numerical simulation process, as well as achieve the higher accuracy of the temperature field data on the basis of the convergence of the flow field.

3. Result Analysis and Discussion

3.1. Internal Circulation Water Cloud Diagram

The internal circulating water has a cooling effect on the roller during the entire centrifugal fiber forming process, which is of great significance in improving the roller life and ensuring the normal operation of the centrifugal fiber forming process. The internal circulating water temperature cloud diagram is shown in Figure 7.
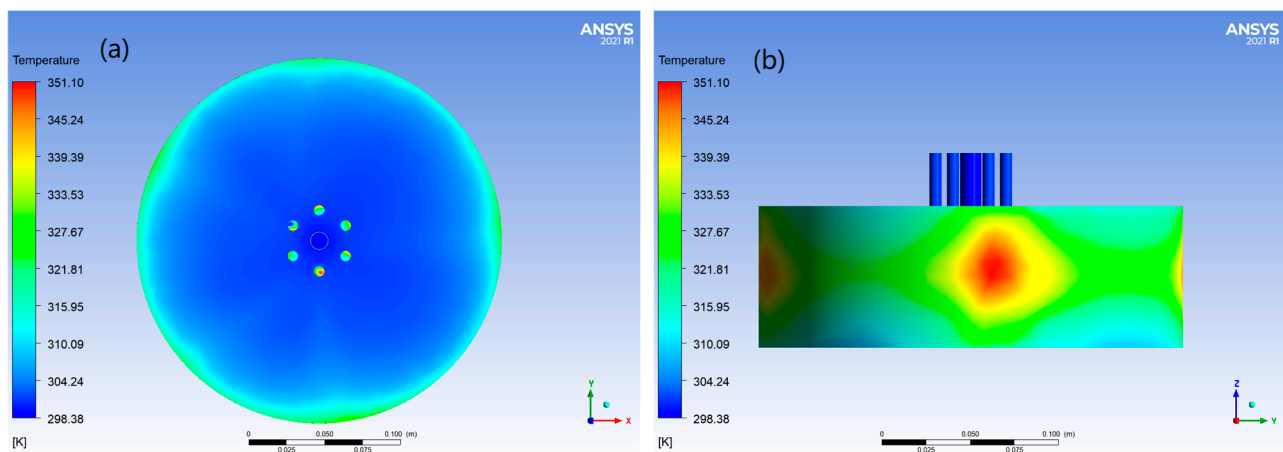
Figure 7. Temperature nephogram of internal circulating water (**a**) inlet and outlet; (**b**) side.

From Figure 7a, it can be seen that the inlet temperature remains at the set temperature of 25 °C. During the entire centrifugal fiber forming process, water absorbs the heat on the roller, so the outlet temperature increases and the average temperature increases by 6 °C. As shown in Figure 7b, the side that directly contacts the roller wall absorbs more heat and has a higher temperature, while the part that does not directly contact the roller wall has a lower temperature. Water is constantly circulating, so it can continuously carry away heat to maintain the normal progress of the entire process.

3.2. Roller Temperature Cloud Map

The roller is the main piece of equipment in the centrifugal fiber forming process and plays a decisive role in whether the process can proceed normally. The temperature cloud map of the roller is shown in Figure 8.
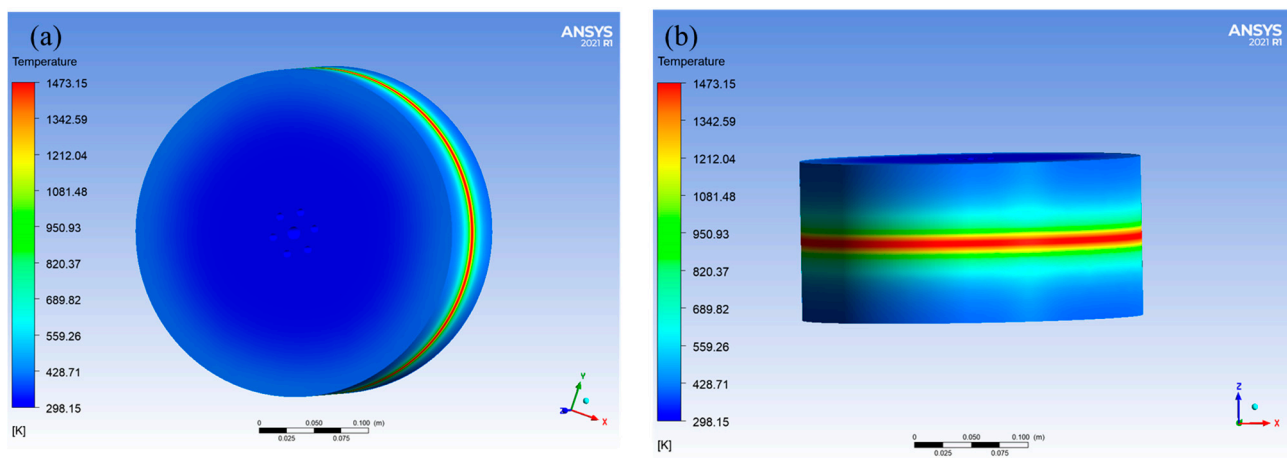

Figure 8. Roller temperature nephogram (**a**) inner end face; (**b**) roll surface.

From Figure 8a, it can be seen that the inner surface is far from the slag and has a small temperature influence, but the temperature also slightly increases. From Figure 8b, it can be seen that the temperature at the direct contact area between the roller and the slag is high, gradually diffusing towards the upper and lower walls, with a diminishing temperature influence. In production, the part where the slag contacts the roller is most affected by the temperature as shown in Figure 8b. Although internal circulating water can carry away a large amount of heat, this part still has the highest temperature compared to the other parts. If the slag temperature is too high, it will cause changes in the structural strength of this part, affecting the normal production process. Therefore, the slag temperature should be controlled within a reasonable range.

3.3. Effect of Slag Temperature on Heat Transfer of Roller

The heat transfer to the roller was studied by changing the slag temperature to 1500 °C, 1525 °C, 1550 °C, 1575 °C, and 1600 °C. The temperature cloud map corresponding to the roller under the five different working conditions is shown in Figure 9.

As shown in Figure 9, as the temperature of the slag increases, the temperature of the roller surface in contact with the slag also increases, resulting in a more pronounced impact on the temperatures at both ends of the roller. The average temperature of the roller surface in contact with the slag and the average temperature of the entire roller surface are shown in Table 3.
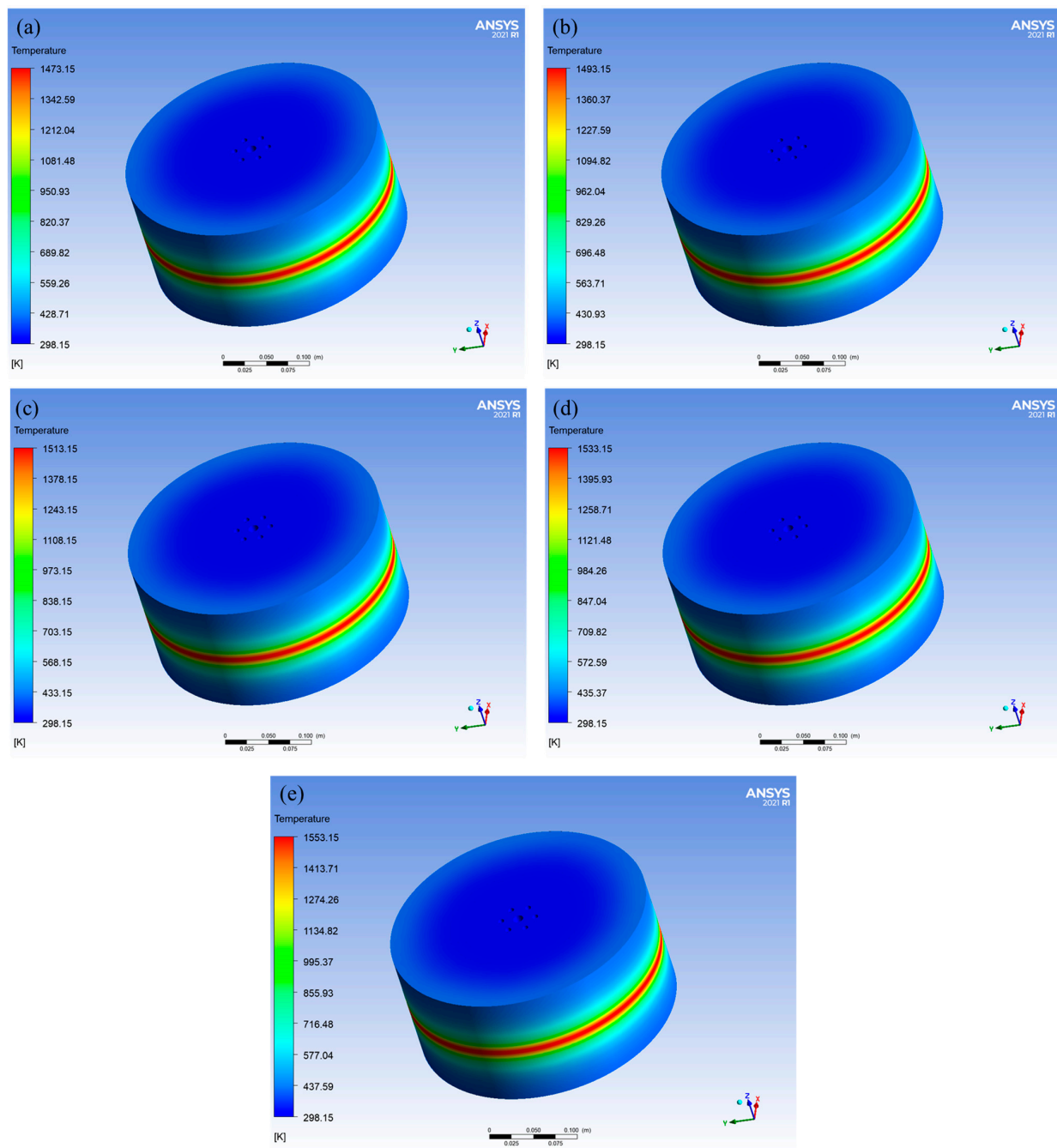
Figure 9. Cloud diagram of roller with different slag temperature (**a**) 1500 °C; (**b**) 1525 °C; (**c**) 1550 °C; (**d**) 1575 °C; (**e**) 1600 °C.

Table 3. Roller surface temperature under different slag temperature.

Slag Temperature/°C	Average Temperature of the Part in Contact with Slag/°C	Average Temperature of the Entire Roller Surface/°C
1500	1074.26	600.14
1525	1093.34	609.98
1550	1111.23	619.56
1575	1129.12	629.65
1600	1147.01	639.48

It can be seen that the maximum and average temperatures of the roller surface are different under the five working conditions. The variations in the average temperature of the roller surface with the slag temperature is shown in Figure 8.

It can be seen from Figure 10 that the average temperature change in the part in contact with the slag is approximately a straight line. By fitting it with a linear function, the growth rate in the figure is 0.9064, that is, when the temperature of the slag increases by 1 °C, the temperature of the roll surface in contact with the slag increases by 0.91 °C; similarly, the average temperature change growth rate of the roller surface is 0.49, which means that when the slag temperature increases by 1 °C. The average temperature of the entire roller surface increases by 0.49 °C.
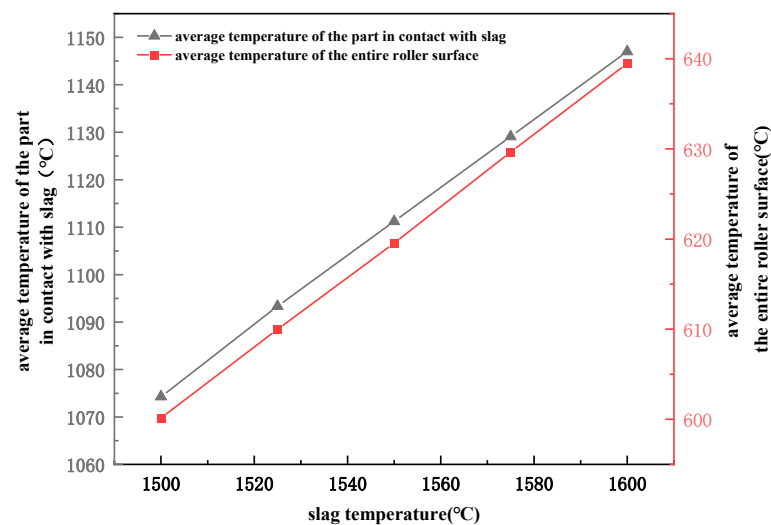

Figure 10. Changes in the average temperature of the contact part with the slag and the average temperature of the entire roller surface under different slag temperatures.

3.4. Effect of Slag Roller Surface width on Heat Transfer of Roller Wheels

The heat transfer of the slag to the roller was studied by keeping the slag temperature at 1500 °C and changing the slag widths to 8 mm, 11 mm, 14 mm, 17 mm, and 20 mm. The temperature cloud map corresponding to the roller under the five different working conditions is shown in Figure 11.

From Figure 11, it can be seen that the highest temperature on the roller surface does not change with the width of the slag on the roller surface, but as the width of the slag on the roller surface increases, the impact on the upper and lower wall temperatures at the direct contact area between the roll and the slag increases. With a larger slag width, the range of the high-temperature zone in the middle is larger, and the heat is transferred to both sides over a wider range, resulting in a greater impact on the temperatures on both sides. The average temperature of the roller surface at the contact area of the slag and the average temperature of the entire roller surface under these five different slag widths are shown in Table 4. The changes are shown in Figure 12.

Table 4. Roller surface temperature under different slag film widths.

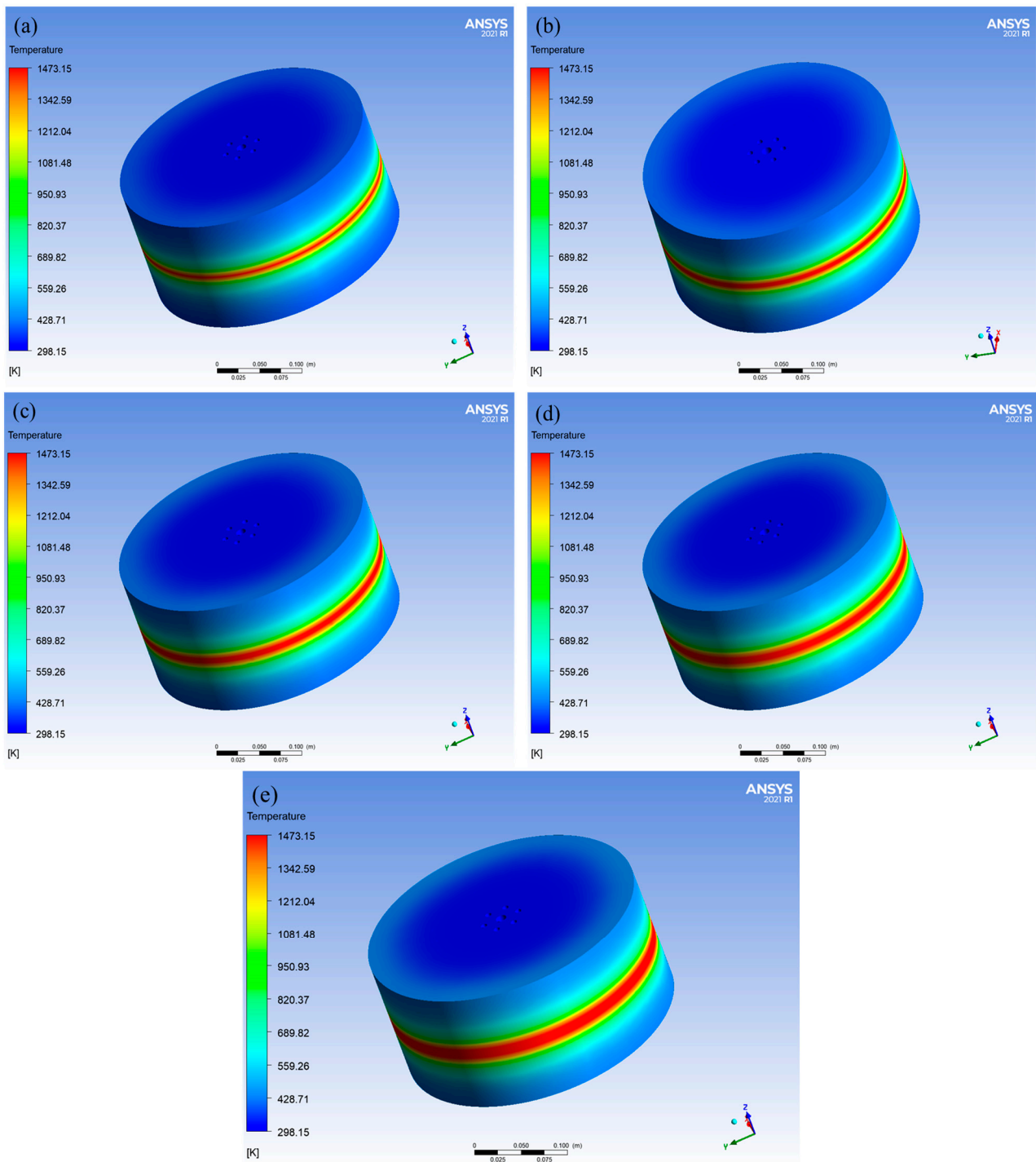| Width of Slag Film/mm	Average Temperature of the Part in Contact with Slag/°C	Average Temperature of the Entire Roller Surface/°C
8	1023.32	544.68
11	1073.89	600.14
14	1074.24	604.11
17	1074.26	622.98
20	1103.89	672.34

Figure 11. Cloud diagram of roller with different slag widths (**a**) 8 mm; (**b**) 11 mm; (**c**) 14 mm; (**d**) 17 mm; (**e**) 20 mm.

As shown in Figure 12, as the width of the slag increases, the average temperature of the roller surface in contact with the slag and the average temperature of the entire roller surface show an upward trend. However, when the width of the slag is 11 mm, 14 mm, or 17 mm, the average temperature of the part in contact with the slag is not significantly different. Therefore, during production, the width of the slag on the roller surface should be controlled to be between 11 and 17 mm to reduce the impact of temperature fluctuations on the roller and extend its service life.
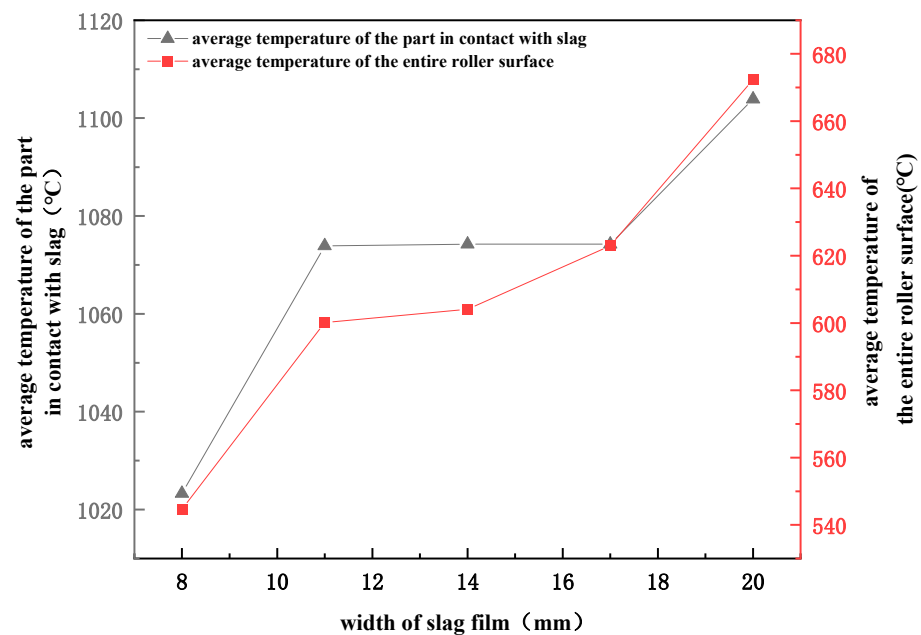
Figure 12. Changes in the average temperature of the roller surface in contact with the slag and the average temperature of the entire roller surface under different slag film widths.

3.5. Effect of Slag Thickness on Heat Transfer of Roller

The thickness of the boundary layer was changed to 0.91 mm, 0.94 mm, 0.97 mm, 1 mm, and 1.06 mm, and the influence on the heat transfer of the roller was studied. The impact of the different boundary layer thicknesses on the average roller surface temperature is recorded in Table 5.

Table 5. Roller surface temperature under different slag thicknesses.

Slag Thickness/mm	Average Temperature of the Part in Contact with Slag/°C	Average Temperature of the Entire Roller Surface/°C
0.91	1074.57	600.70
0.94	1074.31	600.24
0.97	1074.29	600.17
1.00	1074.20	600.02
1.03	1074.26	600.14
1.06	1074.36	600.38

From Table 5, it can be seen that the average temperature of the roller surface is different for the six different slag thicknesses. As the slag thickness increases, the average temperature of the part in contact with the slag and the average temperature of the entire roller surface first decrease and then increase. When the slag thickness is greater than 1 mm, the average temperature of the part in contact with the slag and the average temperature of the entire roller surface slightly increases. The variation in the average temperature of the roller surface with the slag thickness is shown in Figure 13.

As shown in Figure 13, a turning point appears at a slag thickness of 1 mm, so in actual production, the slag thickness should be less than 1 mm. The thickness of the slag is related to the roller speed and the ratio of the raw material. When the raw material composition is determined, the thickness of the boundary layer can be changed by adjusting the roller speed so that the temperature of the roller in contact with the slag is at a lower level, thus extending the service life of the roller.
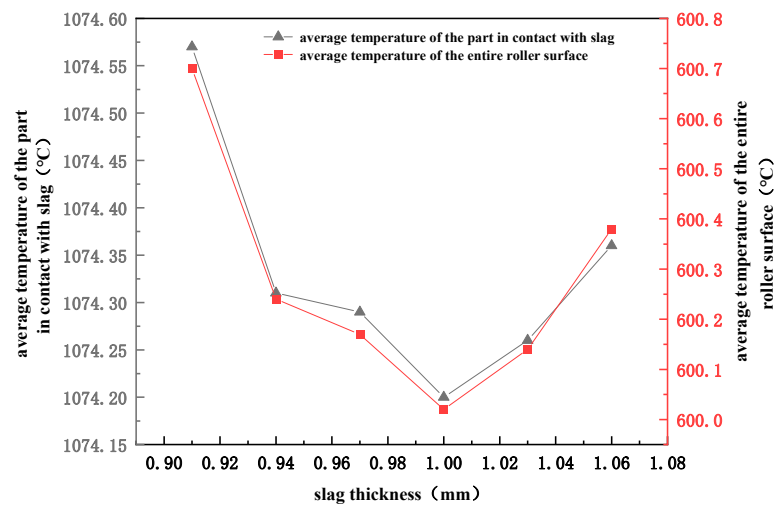
Figure 13. Variation in the average temperature of the contact part with the slag and the average temperature of the roller surface with the thickness of the slag.

4. Conclusions

This article conducts numerical simulation research on the heat transfer between the roller and slag during the centrifugal fiber forming process of the synergistic preparation of ceramic fibers from dust removal ash and fly ash. It explores the influence of internal circulating water on the heat transfer between the roller and slag, and analyzes the heat transfer changes of different slag temperatures, slag widths, and slag thicknesses during the centrifugal fiber forming process. The main conclusions are as follows:

- Internal circulating water has a significant impact on the normal operation of the centrifugal fiber forming process, and cooling with circulating water can ensure that the roller surface temperature is within a reasonable range. The simulation results show that there is a strong heat transfer between the rollers and the slag and circulating water, resulting in an increase in the outlet water temperature by about 6 °C compared to the inlet temperature, which ensures the normal production;

- The heat transfer process between the roller and the slag is uneven, with the highest temperature in the contact area between the roller and the slag, and then gradually spreading towards the upper and lower walls. The part that is most affected by temperature is the contact between the slag and the roller surface. If the slag temperature is too high, it will cause changes in the structural strength of the roller, thereby affecting the progress of production. Therefore, controlling the temperature of the slag falling onto the roller surface within a reasonable range is the key to ensuring normal production. At the same time, according to the simulation data, the manufacturer upgraded the production equipment by moving the rollers back and forth at regular intervals to change the contact surface between the slag and the rollers, which significantly improved the service life of the rollers.

- When the temperature of the slag increases by 1 °C, the temperature of the roller surface in contact with the slag increases by 0.91 °C. The simulation data show that the slag temperature, slag roller width, and the boundary layer thickness will have an impact on the roller temperature. In actual production, the slag outlet size can be adjusted to control the slag roller width to be between 11 and 17 mm to keep the temperature of the roller in contact with the slag part of the roller stable; by controlling the roller speed, the thickness of the slag can be increased or decreased, keeping the temperature of the contact part between the slag and the roller at the lowest level, reducing the impact of high temperatures on the strength of the roller, and extending the service life of the roller.

References

1. Ran, X.; Zou, H.H.; Sun, H.W.; Ye, Y.F. The effect of heat treatment on the interface bonding characteristics and carbon fiber structure of coated carbon fibers. *J. Mater. Heat Treat.* **2015**, *36*, 136–140. [CrossRef]
2. Wang, Q.; Zhao, B.; Han, X.G. Properties and Preparation of Ceramic Fibers. *China Ceram.* **2019**, *55*, 10–18+26. [CrossRef]
3. Cooke, T.F. Inorganic Fibers—A Literature Review. *J. Am. Ceram. Soc.* **1991**, *74*, 2959–2978. [CrossRef]
4. Ishikawa, T. Advances in Inorganic Fibers. *Adv. Polym. Sci.* **2005**, *178*, 109–144. [CrossRef]
5. Li, J.; Zhang, L.L.; Zhao, G.Z.; Cang, D.Q. Pilot practice of directly modifying blast furnace slag to prepare mineral wool fibers. *Iron Steel* **2017**, *52*, 99–103. [CrossRef]
6. Zhang, Z.Q.; Zhang, Y.Z.; Xing, H.W. Analysis of slag centrifugal fiber formation test and its influencing factors on fibrosis. *Steel* **2017**, *52*, 69–74. [CrossRef]
7. Guo, Z.Y.; Yu, P.X.; Ouyang, H. The instability of flow around cylinder shear layer based on large eddy simulation. *J. Shanghai Jiaotong Univ.* **2021**, *55*, 924–933. [CrossRef]
8. Qiu, R.D.; Wang, J.Z.; Huang, R.F. Application of improved physical fusion neural networks to Rayleigh-Taylor instability problems. *Chin. J. Theor. Appl. Mech.* **2022**, *54*, 2224–2234.
9. Bizjan, B.; Širok, B.; Govekar, E. Nonlinear Analysis of Mineral Wool Fiberization Process. ASME. *J. Comput. Nonlinear Dynam.* **2015**, *10*, 21005. [CrossRef]
10. Lin, Y.H.; Li, F.; Zhang, D. A rigid clamping model for the multiple bending forming process of four roller wheels. *J. Fudan Univ.* **2002**, *5*, 495–500. [CrossRef]
11. Jia, C.L.; Shen, Y.R.; Qian, S.Q.; Li, Y.P. 2Cr13 Heat Treatment Process for Finishing Cold Roll Wheels. *Hot Work. Process* **2014**, *43*, 158–160. [CrossRef]
12. Chen, J.; Yan, W.J. Design and finite element analysis of roller components for powder mills. *Mech. Electr. Eng. Technol.* **2021**, *50*, 212–215.
13. Ma, W.X.; Yu, H.J.; Liu, Y.Y.; Qian, C.F. Numerical simulation of heat transfer process between rolling film and cooling drum. *J. Beijing Univ. Chem. Technol.* **2020**, *47*, 84–92. [CrossRef]
14. Chang, L.L.; Liu, Y.; Li, H.R.; Guan, X.R. Numerical simulation study on temperature field of hydrophilic coated aluminum foil water-cooled rolls. *J. Nanjing Univ. Technol.* **2020**, *44*, 733–738. [CrossRef]
15. Li, F.S.; Wang, S.H.; Li, X.X.; Lin, Y.H.; Sun, Y. Numerical simulation of the cooling process of plastic film on a casting roller. *Plast. Technol.* **2011**, *39*, 35–38.
16. Li, Y.K.; Yang, Y.; Song, Y.M. Numerical Simulation of Heat Flow and Temperature Field of Amorphous Belt Cooling Rollers. *Rare Met. Mater. Eng.* **2017**, *46*, 917–922.
17. Wu, S.X. Research on Temperature Field and Stress Field of New Type of Cooling Rolls for Continuous Casting of Slabs. Master's Thesis, Chongqing University, Chongqin, China, 2022. [CrossRef]
18. Dai, W. Temperature field analysis of continuous casting roll bearing housing based on ANSYS. *J. Chang. Univ.* **2014**, *11*, 59–61+4. [CrossRef]
19. Li, S.D. Thermal Structure Coupling Analysis of Casting Roll Sleeve and Its Fatigue Life Study. Master's Thesis, Zhongnan University, Changsha, China, 2007.
20. Yang, B.L. Navier-Stokes equations and generalized laminar flow—The first class dynamic equations of fluid mechanics and their application conditions. In Proceedings of the 16th National Hydrodynamics Seminar, Zhuhai and Macau, China, 17–22 November 2002; pp. 181–196.
21. Zhao, C.L. How to distinguish laminar flow and turbulence. *Coll. Phys.* **1993**, *7*, 16–17+20. [CrossRef]